Proc. of IEEE ISPLC 2013

# Cyclic Block FMT Modulation for Broadband Power Line Communications

Andrea M. Tonello[1,2] and Mauro Girotto[1]
[1]Wireless and Power Line Communications Lab, University of Udine, Italy
[2]WiTiKee s.r.l., Udine, Italy
e-mail: {tonello, mauro.girotto}@uniud.it
web: www.diegm.uniud.it/tonello/wiplilab, www.witikee.com

***Abstract*—A novel multi-carrier modulation scheme for broadband power line communication (PLC) is presented. The novel architecture is based on the Filtered Multitone (FMT) modulation concept. However, the novel modulation scheme uses the circular convolution instead of the linear convolution in the filtering operations. We refer to this new architecture as Cyclic Block Filtered Multitone Modulation (CB-FMT). CB-FMT can benefit from the high sub-channel frequency confinement and the design of an orthogonal prototype pulse is simplified w.r.t. conventional FMT. A simple frequency domain equalizer can be deployed in frequency selective channels. Furthermore, CB-FMT can offer high frequency notching capability which is an important requirement in PLC to fulfill EMC norms. Numerical results show that CB-FMT has higher achievable rate than OFDM for the same number of data sub-channels.**

## I. Introduction

Nowadays, high data rate broadband power line communication (PLC) exploit multi-carrier modulation schemes. Typical power line channels exhibit high frequency selectivity. In time domain, this selectivity is translated into long channel impulse responses. The time dispersion introduces significant inter-symbol interference that requires complex equalization techniques. In multi-carrier modulation schemes, also referred to as filter bank modulation, the wide band channel is partitioned into a number of narrow band sub-channels. Each sub-channel has a more flat frequency response so that the equalization task is simpler than in single-carrier modulations.

One of the most popular multi-carrier modulation techniques is orthogonal frequency division multiplexing (OFDM) [1]. This modulation scheme is widely adopted in different scenarios, e.g. for wireless, in the digital subscriber line and PLC systems. Several PLC systems deploy OFDM both for narrow band (NB) and broadband (BB) applications. NB-PLC operates at the lower frequencies, e.g., in Europe NB-PLC operates in the 3-148.5 kHz CENELEC bands. Two relevant industrial standards are PRIME [2] and G3-PLC [3]. BB-PLC operates in the 2-30 MHz band and it is intended for high-data rate communications, e.g., the HomePlug AV [4] system.

An alternative multi-carrier scheme to OFDM is Filtered Multitone Modulation (FMT) [5]. In contrast to OFDM, where the time domain confinement is preferred, FMT is characterized by high frequency confinement of the sub-channels. When the sub-channel frequency confinement is high, the inter-carrier interference between different sub-channels is lower. In addition, the out-of-band interference is reduced. This aspect has an important implication in BB-PLC. In fact, in the 2-30 MHz band there are several parts of the spectrum where the power of the transmitted signal must be reduced (or totally notched) to generate low emissions and allow the coexistence with other systems, e.g., radio amateur systems. If the sub-channels have high frequency confinement, the number of notched sub-channels that need to be notched will be reduced w.r.t. OFDM. This implies that the data rate penalty is smaller.

In conventional FMT modulation, to obtain high sub-channel frequency confinement, long prototype pulses have to be used. This may increase the implementation complexity. In this paper we present a novel modulation scheme that aims at simplifying the pulse design and reduce the complexity. We replace the linear convolutions of the conventional FMT scheme with circular convolutions. Furthermore, we group the sub-channel data sequences in blocks. We refer to this novel system as Cyclic Block Filtered Multitone Modulation (CB-FMT). In section II, we describe the conventional FMT and the OFDM systems. In Section III, we present the CB-FMT scheme. First, we show how to design a prototype pulse that renders CB-FMT orthogonal. Then, we focus on obtaining orthogonality in frequency selective channels. In Section IV we derive the Power Spectral Density (PSD) of the transmitted signal and we discuss notching to respect EMC masks. In Section V, we compare the CB-FMT with OFDM in terms of maximum achievable rate. Finally, in Section VI, the conclusions follow.

## II. Multi Carrier Modulation

In a multi-carrier modulation scheme, the high-data rate sequence, $a(n)$, is split into $K$ low data-rate sequences, denoted with $a^{(k)}(N\ell)$, $k = 0, ..., K-1$. The available channel bandwidth is partitioned in $K$ sub-channels, one for each low rate sequence. This technique allows us to simplify the equalization task at the receiver. Several modulation schemes have been proposed. We focus on Filtered Multitone Modulation (FMT) and on Orthogonal Frequency-Division Multiplexing (OFDM). These schemes have uniform sub-channel spacing and identical sub-channel pulse shape.

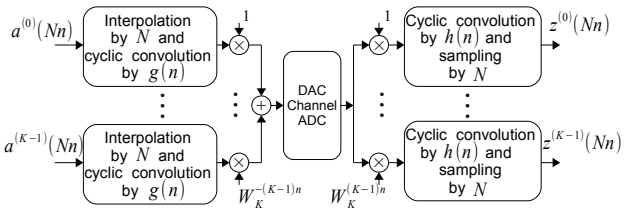


Fig. 1. CB-FMT transceiver scheme.

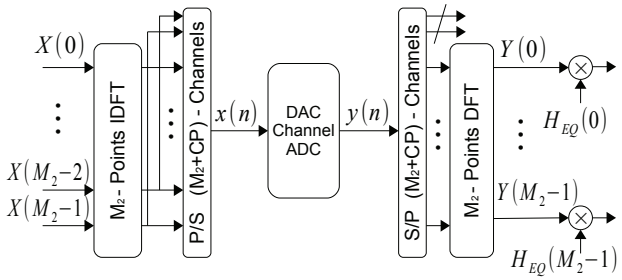


Fig. 2. Outer cyclic extension with frequency domain equalizer.

### A. FMT Modulation

In conventional FMT, each low rate sequence $a^{(k)}(N\ell)$ is interpolated by a factor $N$ and, then, filtered with the prototype pulse $g(n)$. The $K$ filtered signals are translated in frequency by a complex exponential multiplication. The $K$ sub-channel signals are then summed to obtain the transmitted signal $x(n)$, expressed as

$$x(n) = \sum_{k=0}^{K-1} \sum_{\ell \in \mathbb{Z}} a^{(k)}(N\ell) g(n - N\ell) W_K^{-nk}, \qquad (1)$$

where $W_K^n = e^{-i2\pi n/K}$ is the complex exponential. The signal in (1) is digital-to-analog converted and then transmitted over a power line dispersive channel. At the receiver side, the signal is low-pass filtered and, then, analog-to-digital converted. The received signal, in discrete time, can be express as

$$y(n) = x * h_{CH}(n) + \eta(n), \qquad (2)$$

where $*$, $h_{CH}(n)$ and $\eta(n)$ are the linear convolution operator, the discrete time equivalent channel impulse response and the background colored Gaussian noise, respectively. After demodulation of (2) with a bank of complex exponential multiplicators, the obtained sub-channel signals are filtered with $h(n)$ and finally they are sampled by $N$. The output signal for the $k$-th sub-channel can be written as

$$z^{(k)}(Nn) = \sum_{\ell \in \mathbb{Z}} y(\ell)\, W_K^{\ell k}\, h(Nn - \ell). \qquad (3)$$

In FMT the prototype pulse is confined in the frequency domain, e.g. the root raised cosine pulse is a common choice.

### B. OFDM Modulation

The OFDM scheme can be seen as an FMT scheme where $N = K$ and the prototype pulse is the rectangular function, i.e. $g(n)$ is equal to 1 for $n \in [0, N-1]$ and 0 otherwise. Due to the rectangular pulse shape, the transmitted signal (1) can be efficiently obtained with a $K$-points Inverse-Discrete Fourier Transform (IDFT)

$$x(n) = \frac{1}{K} \sum_{k=0}^{K-1} a^{(k)}(N\ell) W_K^{-nk}, \quad N\ell \le n < (\ell+1)N. \quad (4)$$

The output of the IDFT stage is extended with a cyclic prefix (CP) of $\mu$ samples. At the receiver, we discard the CP and we apply a Discrete Fourier Transform (DFT). Finally, a 1-tap MMSE equalization is performed. if the CP is greater than the maximum time dispersion introduced by the channel, there will not be inter-symbol interference (ISI). Differently from FMT, the prototype pulse is not well confined in the frequency domain.

## III. Cyclic Block FMT Modulation

The idea behind our novel multi-carrier modulation scheme is to substitute the linear convolution in (1) with a circular convolution. Then, we group and process the low rate sequence $a^k(N\ell)$ in blocks of $L$ symbols. We refer to this modulation scheme as Cyclic Block Filtered Multitone Modulation (CB-FMT). The CB-FMT scheme is depicted in Fig. 1. The transmitted signal can be rewritten as

$$x(n) = \sum_{k=0}^{K-1} \sum_{\ell=0}^{L-1} a^{(k)}(N\ell) g((n - N\ell))_{M_2} W_K^{-nk}, \qquad (5)$$
$$n \in \{0, \cdots, M_2 - 1\},$$

where $g((n-N\ell))_{M_2}$ is the periodic repetition with period $M_2$ of the prototype pulse $g(n)$ shifted by $N\ell$, i.e. the cyclic shift $g((n - N\ell + M_2))_{M_2} = g(n - N\ell)$. We assume the prototype pulse to be a casual FIR filter with a number of samples equal to $M_2 = LN$. If $g(n)$ has less than $M_2$ samples, we will extend the impulse response to $M_2$ with zero-padding.

Similarly to the transmitter, at the receiver we replace the linear convolution with the circular convolution in (3). Thus, we obtain

$$z^{(k)}(Nn) = \sum_{\ell=0}^{M_2-1} y(\ell) W_K^{\ell k} h((Nn - \ell))_{M_2}, \qquad (6)$$
$$n \in \{0, \cdots, L-1\},$$

where $h((Nn-\ell))_{M_2}$ denotes the cyclic shift of $h(n)$, i.e. $h((Nn - \ell + M_2))_{M_2} = h(Nn - \ell)$.

### A. Prototype Pulse Design

To design the prototype pulse, we work in the frequency domain by exploiting the DFT of the transmitted signal $x(n)$. First, we define $Q$ such that $M_2 = LN = KQ$. Then, we compute a $M_2$-points DFT of (5), i.e. $X(i) = \sum_{n=0}^{M_2-1} x(n) W_{M_2}^{ni}$. We obtain

$$X(i) = \sum_{k=0}^{K-1} A^{(k)}(i - Qk) G(i - Qk), \qquad (7)$$

where $A^{(k)}(i)$ and $G(i)$ are the $L$-points DFT of the $L$ symbols $a^{(k)}(N\ell)$, $\ell \in \{0, \ldots, L-1\}$ and the $M_2$-points DFT of the

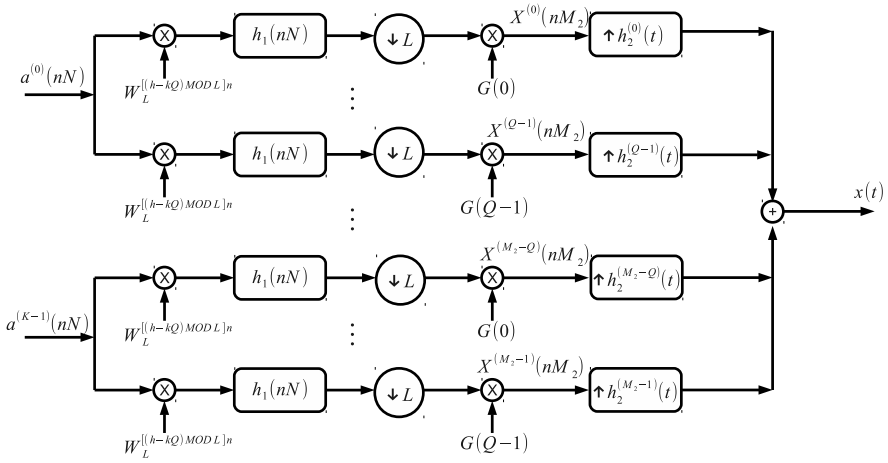


Fig. 3. Linear equivalent model for CB-FMT transmitter.

prototype pulse $g(n)$, respectively. From the previous relation, we note that if $G(i) = 0$ for $i \in \{Q, \ldots, M_2 - 1\}$, (7) can be simply rewritten as

$$X(i) = A^{(k)}(i - Qk)G(i - Qk), \quad i \in \{Qk, \cdots, Q(k+1) - 1\}, \quad k \in \{0, \cdots, K-1\}. \tag{8}$$

Under this assumption, there is no inter-channel interference (ICI) due to the pulse frequency confinement.

In particular, in this paper we choose the prototype pulse to be a rectangular window in the frequency domain. Other pulse shapes are designed in [6]. Thus, $G(i)$ is equal to 1 for $i \in \{0, \ldots, Q-1\}$ and 0 otherwise. Consequently, at the receiver, we can rewrite (6) as

$$z^{(k)}(Nn) = \sum_{p=0}^{L-1} Z^{(k)}(p - Qk) W_L^{-(p-Qk)n}. \tag{9}$$

The signal $Z^{(k)}(p - Qk)$ can be written as

$$Z^{(k)}(p - Qk) = \sum_{q=0}^{N-1} Y(p + Lq) H(p + Lq - Qk), \tag{10}$$

where $Y(i)$ and $H(i)$ are the $M_2$-points DFT of the received signal $y(n)$ and the $M_2$-points DFT of the prototype pulse $h(n)$, respectively. We choose the prototype pulse $h(n)$ according to the matched filter concept, i.e. $g(n) = h^*(-n)$. In the particular case of this paper, we have simply $H(i) = G(i)$. Under this assumption, the CB-FMT filter bank is orthogonal and there is no inter-symbol interference (ISI) between the $L$ symbols of each block due to the Nyquist criterion.

### *B. Orthogonality with Frequency Selective Channels*

The design described in the previous section renders CB-FMT orthogonal when the channel is ideal. A real power line frequency-selective channel introduces inter-block interference (IBI) due to the linear convolution in (2). To prevent this, similarly to OFDM, we may apply a cyclic prefix (CP) to the transmitted signal block, as shown in Fig. 2. In this way, provided that the CP is longer than the channel duration, the linear convolution in (2) becomes a circular convolution. Therefore, the $M_2$-points DFT outputs of the received signal can be simply written as

$$Y(p) = X(p) H_{CH}(p) + N_w(p), \tag{11}$$

where $H_{CH}(p)$ and $N_w(p)$ are the $M_2$-points DFT of the channel impulse response and the $M_2$-points DFT of the background colored noise samples, respectively. This allows us to use a simple MMSE equalizer. In detail, the outputs of the DFT of the received signal (11) are weighted by the coefficients

$$H_{EQ}(p + kQ) = \frac{H^*_{CH}(p + kQ)}{|H_{CH}(p + kQ)|^2 + \frac{M_w(p+kQ)}{G(p)}}, \quad p \in \{0, \ldots, Q-1\}, \quad k \in \{0, \ldots, K-1\}, \tag{12}$$

where $M_w(p + kQ)$ is equal to $E[|N_w(p + kQ)|^2]$ and $E[\cdot]$ is the expectation operator. Then, further processing via IDFT brings the signals into time domain.

## IV. PSD Related Aspects

Broadband PLC generally operates in the band 2-30 MHz [7]. Transmission above 30 MHz is possible, but the Electromagnetic compatibility (EMC) limits are more stringent than the limits in the band below 30 MHz. In the 2-30 MHz range there are several sub-bands dedicated to other communication systems, e.g. to amateur radio. A spectrum notching mask has to be fulfilled by the Power Spectral Density (PSD) of the transmitted signal to grant coexistence. In the notching frequencies, the PSD level must be less than $-80$ dBm/Hz. Otherwise, the PSD limit is set to $-50$ dBm/Hz.

In the following we derive an analytic expression for the PSD of CB-FMT. The PSD of OFDM modulation is discussed in [8], [9]. In Fig. 3, we show a linear model for the CB-FMT transmitter, which is valid when the relation (8) is satisfied. The figure shows that each sub-channel signal is modulated with a complex exponential and then it is processed by a

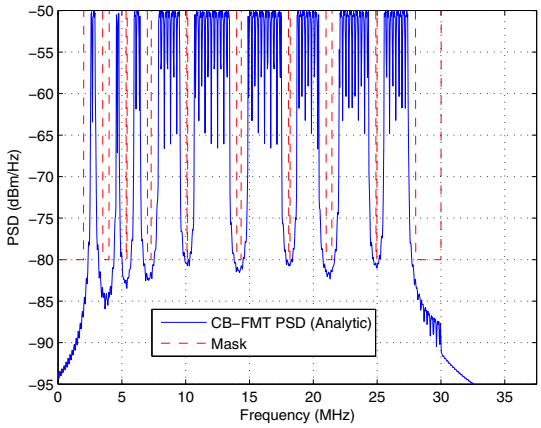


Fig. 4. Power Spectral Density of CB-FMT transmitted signal and the HomePlug notching mask.

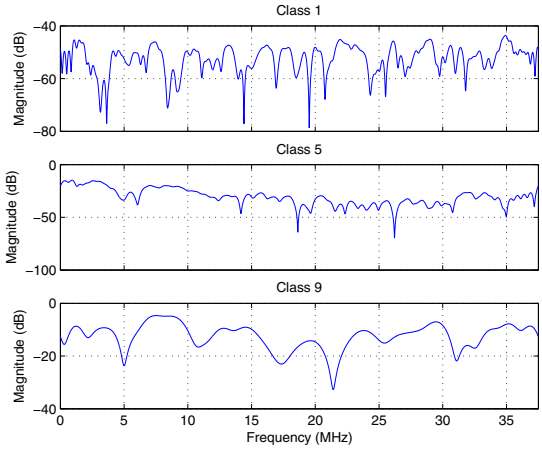


Fig. 5. Magnitude of three channel realizations generated with the statistical top-down model.

synthesis filter bank with pulse response $h_1(Nn)$ equal to 1 for $n \in \{0, \ldots, L-1\}$ and 0 otherwise. The output of each filter is sampled by $L$ and weighted with the prototype pulse frequency response coefficients. Finally, an interpolation filter with impulse response $h_2^{(a)}(t) = \text{rect}\left(\frac{t}{(M_2+\mu)T}\right) e^{-i2\pi at/(M_2 T)}$, $t \in \mathbb{R}$, where $T$ is the sampling period, is applied.

If we assume the data symbols to be independent with zero mean, the PSD expression can be obtained by computing the correlation of $x(t)$

$$r_x(t,\tau) = E\left[x(t+\tau)^* x(t)\right]. \tag{13}$$

Due to the interpolation filter $h_2^{(a)}(t)$, the transmitted signal is cyclo-stationary so that (13) is periodic [10], i.e. $r_x(t + T_0, \tau) = r_x(t, \tau)$, where $T_0 = (M_2 + \mu)T$. Thus, we evaluate the mean correlation $\overline{r_x(\tau)} = \frac{1}{T_0}\int_0^{T_0} r_x(t,\tau)\, dt$. After some algebraic manipulation we obtain the mean PSD expression as follows

$$\overline{P_x(f)} = P_1(f) + P_2(f), \tag{14}$$

$$P_1(f) = \frac{L}{T_0}\sum_{k=0}^{K-1}\sum_{q=0}^{Q-1} |G(q)|^2 \left|G_P(f - f_{k,q})\right|^2, \tag{15}$$

$$P_2(f) = \frac{2L}{T_0}\sum_{k=0}^{K-1}\sum_{q=0}^{Q-L-1} \text{Re}\left\{G(q)\left(G(q+L)\right)^* \times G_P(f - f_{k,q})\left(G_P(f - f_{k,q+L})\right)^*\right\}, \tag{16}$$

where $G_P(f) = T_0 \text{sinc}\left(T_0 f\right)$ and $f_{k,q} = T_0(q + kQ)/(M_2 T)$. The PSD comprises the sum of two terms. The first term, $P_1(f)$, represents a sum of a sinc functions, each centered in $f_{k,q}$ and weighed by the prototype pulse frequency response. To understand the meaning of the second term, $P_2(f)$, we may consider (8) and we may focus on $k = 0$

$$X(i) = A^{(0)}(i)G(i), \quad i \in \{0, \cdots, Q-1\}. \tag{17}$$

If $Q > L$, we will have $X(L) = A^{(0)}(L)G(L) = A^{(0)}(0)G(L)$. Thus, the correlation between $X(i)$ and $X(i + L)$ is not null. Equation (16) takes into account this correlation. For the special case of a prototype filter with rectangular frequency response, we have $Q = L$ so that $P_2(f)$ is null. Consequently, the PSD simply becomes $\overline{P_x(f)} = P_1(f)$.

To keep the signal PSD under the mask limits, we need to reduce the transmitted power in some frequencies, such that $\overline{P_x(f)} < P_{mask}(f)$. To fulfill the mask we can appropriately weight the sub-channel pulse frequency response. More precisely, we modulate the amplitude of the pulse frequency response $G(p)$ so that the notching mask is fulfilled. In Fig. 4, we show an example of notching mask and CB-FMT spectrum.

## V. Numerical Results

We evaluate the performance of the proposed CB-FMT scheme in terms of maximum achievable rate and we perform a comparison with the standard OFDM system. We consider transmission over a power line dispersive channel, generated with the statistical top-down channel model presented in [11] and [12]. The model fits a set of large measurement campaign reported in [13] and [14]. The measurement has shown that the channels can be partitioned into nine classes as a function of the average path loss profile. Three representative channel realization belonging to classes 1, 5 and 9 have been used for the simulation and they are reported in Fig. 5.

We model the background noise as additive colored Gaussian noise whose PSD profile decreases following an exponential function

$$PSD_\eta(f) = 28.694\, e^{-0.044 f/10^6} - 107. \quad \text{[dBm/Hz]} \tag{18}$$

The noise model is described in [15].

For both the OFDM and CB-FMT systems we set the sampling frequency $1/T = 37.5$ MHz, as in the HomePlug standard. We choose the cyclic prefix greater than the maximum channel impulse response length. In our case wet set the CP equal to 4 $\mu$s. Furthermore, we impose the PSD mask constraint as described in Section IV and in Fig. 4. To provide a comparison, we evaluate the achievable rate with the Shannon capacity formula. For OFDM modulation, assuming

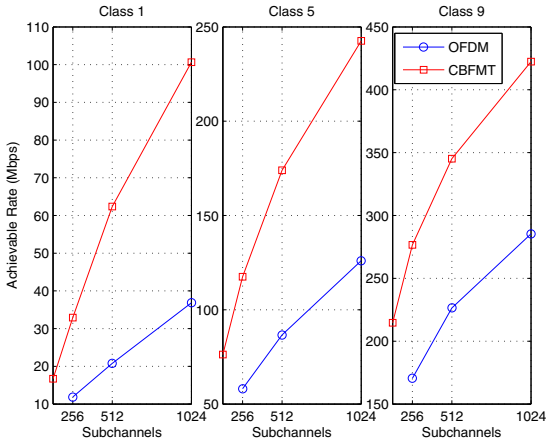


Fig. 6. Achievable rate for CB-FMT and OFDM as a function of sub-channel number.

a CP longer than the channel duration, the achievable rate is given by

$$C_{ofdm} = \frac{1}{(N+\mu)T} \sum_{k=0}^{N-1} \log_2 \left(1 + \frac{P_a(k)}{P_\eta(k)}\right), \qquad (19)$$

where $P_a(k)$ and $P_\eta(k)$ are the output signal power of the $k$-th sub-channel and the output power of noise, respectively. $P_a(k)$ takes into account both the channel attenuation and the signal transmitted power that allows us to fulfill the notching mask. For the CB-FMT system, we can view it as $LK$ equivalent parallel signal transmissions, as shown in Fig. 3. The achievable rate is therefore given by

$$C_{cbfmt} = \frac{1}{(M_2+\mu)T} \sum_{k=0}^{KL-1} \log_2 \left(1 + \frac{P_a(k)}{P_\eta(k) + P_I(k)}\right), \qquad (20)$$

where $P_a(k)$, $P_n(k)$ and $P_I(k)$ are the output signal power of the $k$-th sub-channel, the output power of the noise and the output power of the interference that may be present, respectively. Interference can in fact be present among the $L$ data symbols transmitted in one of the $K$ sub-channels unless Zero-Forcing equalization is implemented.

In our simulation, we have chosen $Q = 4$, $L = Q$, $N = K$. Fig. 6 shows the achievable rate for OFDM and CB-FMT as a function of the number of sub-channels. CB-FMT has better achievable rate for each channel class. This is because CB-FMT has better notching capability and it is capable of exploiting the sub-channel frequency diversity with the use of the sub-channel MMSE equalizer.

Performance gains are attainable with increased complexity. An efficient frequency domain implementation of CB-FMT is proposed in [6] where it is shown that CB-FMT is significantly less complex than conventional FMT assuming the same number of sub-channels and pulse length. Compared to OFDM the complexity of the CB-FMT implementation discussed in this paper, is higher by a factor of 1.4 assuming $K = 1024$ data sub-channels for both systems.

## VI. Conclusions

We have presented a novel multi-carrier system referred to Cyclic Block Filtered Multitone Modulation (CB-FMT). A significant difference and distinctive factor w.r.t. the conventional FMT scheme is in the convolution operation. FMT uses the linear convolution to filter the sub-channel data sequences. Instead, CB-FMT uses the circular convolution. We have discussed the prototype pulse design to obtain an orthogonal CB-FMT filter bank, as well as we have proposed the use of a simple MMSE frequency domain equalizer for frequency selective channels. Then, we have focused on the notching mask problem and we have found an analytic expression for the Power Spectral Density of the transmitted signal.

Finally, numerical results have shown that CB-FMT can provide higher achievable rate than OFDM in typical PLC channels fulfilling severe power spectrum mask constraints. Future work will be focused on he analysis of the computational complexity and on efficient implementation. In addition, we will study the optimization problem of the system parameters as a function of the channel characteristics.

## References


[1] S. Weinstein and P.Ebert, "Data Transmission by Frequency-Division Multiplexing Using the Discrete Fourier Transform," *IEEE Transactions on Communication Technology*, vol. 19, pp. 628 – 634, October 1971.

[2] Draft Standard for PoweRline Intelligent Metering Evolution R1.3E. [Online]. Available: http://www.prime-alliance.org

[3] K. Razazian, M. Umari, A. Kamalizad, V. Loginov, and M. Navid, "G3-PLC Specification for Powerline Communication: Overview, System Simulation and Field Trial Results," in *IEEE International Symposium on Power Line Communications and Its Applications (ISPLC)*, March 2010, pp. 29–318.

[4] Home Plug Alliance. [Online]. Available: www.homeplug.org

[5] G. Cherubini, E. Eleftheriou, and S. Olcer, "Filtered Multitone Modulation for Very High-Speed Digital Subscribe Lines," *IEEE Journal on Selected Areas in Communications*, vol. 20, no. 5, pp. 1016–1028, June 2002.

[6] A. M. Tonello, "A Novel Multi-carrier Scheme: Cyclic Block Filtered Multitone Modulation," in *Proceedings of IEEE International Conference on Communications (ICC 2013)*, June 2013.

[7] H. C. Ferreira, L. Lampe, J. Newbury, and T. G. Swart, *Power Line Communications: Theory and Applications for Narrowband and Broadband Communications over Power Lines*. NY: Wiley and Sons, 2010.

[8] M. T. Ivrlac and J. A. Nossek, "Influence of a Cyclic Prefix on the Spectral Power Density of Cyclo-Stationary Random Sequences," *Multi-Carrier Spread Spectrum*, pp. 37–46, 2007.

[9] T. van Waterschoot, V. Le Nir, J. Duplicy, and M. Moonen, "Analytical Expressions for the Power Spectral Density of CP-OFDM and ZP-OFDM Signals," *IEEE Signal Processing Letters*, vol. 17, no. 4, pp. 371–374, April 2010.

[10] J. Proakis, *Digital Communications*. McGraw-Hill, 2008.

[11] A. M. Tonello, "Wideband Impulse Modulation and Receiver Algorithms for Multiuser Power Line Communications," *EURASIP Journal on Advances in Signal Processing*, pp. 1–14, 2007.

[12] A. M. Tonello, F. Versolatto, B. Bejar, and S. Zazo, "A Fitting Algorithm for Random Modeling the PLC Channel," *IEEE Transactions on Power Delivery*, vol. 27, no. 3, pp. 1477–1484, July 2012.

[13] "PLC Channel Characterization and Modelling," Seventh Framework Programme : Theme 3 ICT-213311 OMEGA, Deliverable D3.2, 2008.

[14] M. Tlich, A. Zeddam, F. Moulin, and F. Gauthier, "Indoor Power-Line Communications Channel Characterization Up to 100 MHz - Part I: One-Parameter Deterministic Model," *IEEE Transactions on Power Delivery*, vol. 23, no. 3, pp. 1392–1401, July 2008.

[15] M. Babic et al., "OPERA Deliverable D5. Pathloss as a Function of Frequency, Distance and Network Topology for Various LV and MV European Powerline Networks," OPERA-IST Integrated Project No 507667, 2005.